ACS OMEGA

Open Access

http://pubs.acs.org/journal/acsodf

Article

Exploiting the (−C−H···C−) Interaction to Design Cage-Functionalized Organic Superbases and Hyperbases: A Computational Study

Anusuya Saha and Bishwajit Ganguly*

Cite This: *ACS Omega* 2023, 8, 38546−38556

Read Online

ACCESS | Metrics & More | Article Recommendations | Supporting Information

ABSTRACT: A set of carbon center-based P-ylidesubstituting bases have been exploited computationally with pentacyclo-[5.4.0.0^{2,6}.0^{3,10}.0^{5,9}]undecane (PCU) and pentacyclo [6.4.0.0^{2,7}.0^{3,11}.0^{6,10}] dodecane (PCD) scaffolds using the B3LYP-D3/6-311+G(d,p) level of theory. The proton affinities calculated in the gas phase are in the range of superbases and hyperbases. The Atomsin-Molecules and Natural Bond Orbital calculations reveal that the −C−H···C− interaction plays a substantial role in improving the basicity, and tuning the −C−H···C− interaction can enhance the basicity of such systems. The free activation energy for proton exchange for PCD and PCU scaffolds substituted with P-ylide is substantially low. The computed results reveal the strength and nature of such − C−H···C− interactions compared to the −N−H···N− hydrogen bonds. The isodesmic reactions suggest that the superbasicity achieved using these frameworks arises from a combination of several factors, such as the ring strain of the bases in their unprotonated form, steric repulsion, and the intramolecular −C−H···C− interaction.

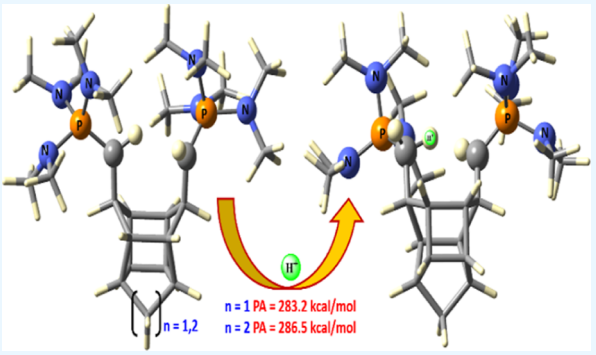

INTRODUCTION

In a multitude of physical, chemical, and biological processes, weak interactions, including both inter- and intramolecular hydrogen bonding, are well documented.[1] These interactions have been exhibited in the molecular arrangement of crystals, crystal engineering, proton-transfer reactions, enzyme catalysis, and in many biological systems.[1] One of the earliest explanations of traditional hydrogen bonding was provided by Linus Pauling.[2] This traditional hydrogen bonding is characterized by the D−H···A interaction, where D represents the hydrogen bond donor, covalently bonded with the H atom, and A acts as the hydrogen bond acceptor.[2−4] In the case of traditional hydrogen bonding, D and A are majorly O, N, F, and Cl. The −O−H···O− hydrogen bonding is widely known from the crystal structure of ice to various oxygen-containing molecules. The −F−H···F− hydrogen bonding contributes to various fluorinated organic compounds in crystal packing and stability.[5] The complementary base pairs of guanine with cytosine and adenine with thymine found in DNA are the most prominent examples of −N−H···O− and −N−H···N− hydrogen bonding. The −N−H···N− type hydrogen bond is also prevalent in various chemical and biological systems, ranging from small organic molecules to the folding of long protein chains.[6,7] This type of hydrogen bonding plays a crucial role in the creation of nitrogen-containing superbases like 1,8-bis(dimethylamino)naphthalene (DMAN) and 1,8-bis-(tetramethylguanidino)naphthalene (TGMN).[8,9] The traditional hydrogen bonds possess energy in the range of ∼12−24 kcal/mol or even higher and are referred to as strong hydrogen bonds.[10,11] These traditional hydrogen bonds often referred to as conventional hydrogen bonds have been studied extensively.[11,12]

However, in the current scenario, the understanding of hydrogen bonding spans a broader range of donors and acceptors, which include electron-rich regions such as π-bonds and alkyl radicals as hydrogen bond acceptors.[1,4,13−16] The existence of a weak −C−H···O− hydrogen bond has been reported in the adenine-thymine base pair along with the −N−H···O− and −N−H···N− hydrogen bonds.[17] The interactions involving the −C−H···N− hydrogen bonding interaction play a significant role in many processes, including catalysis by stabilizing transition states and peptide helical folding.[18] These types of hydrogen bonding interactions are referred to as nonconventional hydrogen bonds and are generally weaker in nature.[19] Nonconventional hydrogen bonding interactions can be classified majorly into four types: (a) hydrogen bonds with −C−H bonds considered as unconventional donors (b)

Received: July 25, 2023
Accepted: September 22, 2023
Published: October 2, 2023

Scheme 1. Naphthalene, PCU, and, PCD Scaffolds Substituted with P and P_2

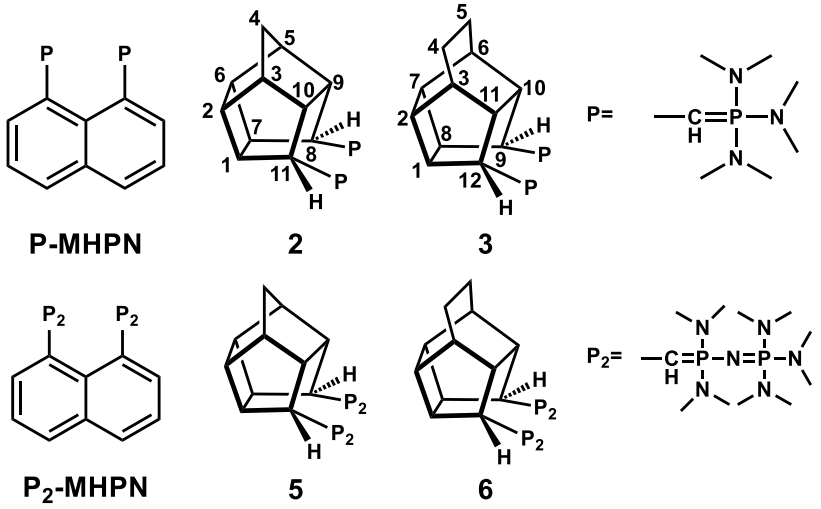

hydrogen bonds with unconventional acceptors, like π-electrons in multiple bonds or within aromatic systems, (c) hydrogen bonds with −C−H···C− (or −C−H···π) systems known as unconventional donors and unconventional acceptors, and (d) dihydrogen bonds.[12,13] It has been reported that when the carbon atom has an excess negative charge, it may participate in hydrogen bonding as a hydrogen bond acceptor. In literature, such −C−H···C− interactions have been examined computationally using carbocations and carbanions with water, acetylene, and methane molecules.[20] The −C−H···C− interaction can be enhanced by using a higher acidic proton donor moiety, such as acetylenes, or by enhancing the basicity of the acceptor.[15] A computational study was performed using the model ylide $H_3N^+-CH_2^-$ with acetylene and methane to demonstrate the strength of hydrogen bonding incorporating the acidic hydrogen in the former molecule.[15] Further, the computational results revealed the strength of hydrogen bonding using (−CH···C−) and CH_4, CH_3X, and CH_2X_2 (X = F, Cl) molecules.[14] In a recent study, it was also found that the −C−H···C− hydrogen bonds assist in substrate binding with proteins.[13] However, the −C−H···C− hydrogen bonds are often considered weaker than typical hydrogen bonds and have received less attention.

Neutral organic nitrogen superbases are known to have broad applications in organic synthesis over ionic bases, since such bases may be utilized under gentle reaction conditions and have greater solubility.[21] Recently, the preparation of such organic superbases have received a lot of attention.[21] Strong neutral bases allow the deprotonation of various weak acids to yield extremely reactive conjugate acids.[21] In this regard, along with the other nitrogen-containing superbases, phosphazenes and phosphatranes have generated curiosity among synthetic organic chemists.[21,22] However, the report indicates that P-ylidic carbon bases, i.e.. phosphorane or its higher analogues may be even more powerful superbases than the phosphazene bases.[23] The computational results suggest that the intrinsic basicity of phosphoranes is greater than that of phosphazenes: for instance, $(Me_2N)_3P{=}CH_2$ (274.5 kcal/mol) has a higher proton affinity (PA) than the equivalent nitrogen containing phosphazene $(Me_2N)_3P{=}NH$ (256.3 kcal/mol) at B3LYP/6-311+G**.[3,22] The P-ylide moieties are less explored in experimental chemistry due to their air sensitivity.[22] The experimental basicity of a series of P-ylides was calculated in THF and acetonitrile solvents;[24] however, there are a few reports which exploited different P-ylides as a substituting group to generate superbases.[22] Tris(dialkylamino)phosphine ylides and their derivatives were synthesized and reported as cyclic ylide bases.[25] The tris(dialkylamino)phosphine ylide is the carbon analogue of Verkade's proazaphosphatrane base, which involves a single ylide group as a proton-capturing unit.[26] However, the synthesis of 1,8-bis(methylylidene-(hexamethyltriamino)phosphorane)naphthalene (**P-MHPN**), was the first report exploiting bisylide substitution (two ylide groups) as a proton-capturing unit.[22] It was anticipated that **P-MHPN** involves fast proton hopping and a dynamic −C−H···C− interaction to achieve superbasicity.[22] The NMR spectroscopic study revealed that in the conjugate acid, the acidic proton hops between the two ylide groups. At a lower temperature, two sets of clearly distinguishable signals for ^1H and ^{31}P spectra were observed. However, at elevated temperature, these signals got merged into a single set of spectra, revealing the dynamic nature of the proton. It has been suggested that the dynamic behavior of the proton is responsible for the higher basicity of bisylide substitution.[22] The computational results reveal that the calculated PA for **P-MHPN** was 277.9 kcal/mol in the gas phase,[22] which is higher than that of the corresponding nitrogen analogue 1,8-bis(hexamethyltriaminophosphazenyl) naphthalene (HMPN, PA = 271.3 kcal/mol).[27] In this work, we have computationally examined the significantly higher basicity of the P-ylide group and the contribution of the [−C−H···C−] interaction to the stability of the conjugate acid. Further, pentacyclo-[5.4.0.0.2,60.3,100^{5,9}] undecane (PCU) and pentacyclo-[6.4.0.0.^{2,7}0.^{3,11}0^{6,10}]dodecane (PCD) scaffolds with P-ylide substitution were used to generate superbases. These scaffolds were also exploited to generate hyperbases with the higher analogue of P-ylide.

COMPUTATIONAL DETAILS

The DFT method incorporating Becke's three-parameter hybrid functional with Lee, Yang, and Parr (B3LYP)[28] correlation and Grimme's third-generation dispersion correction[29] with the 6-311+G(d,p)[30] basis set was used for optimizing all developed systems, and calculations were performed using the Gaussian 09 software package.[31] The

https://doi.org/10.1021/acsomega.3c05401
ACS Omega 2023, 8, 38546−38556

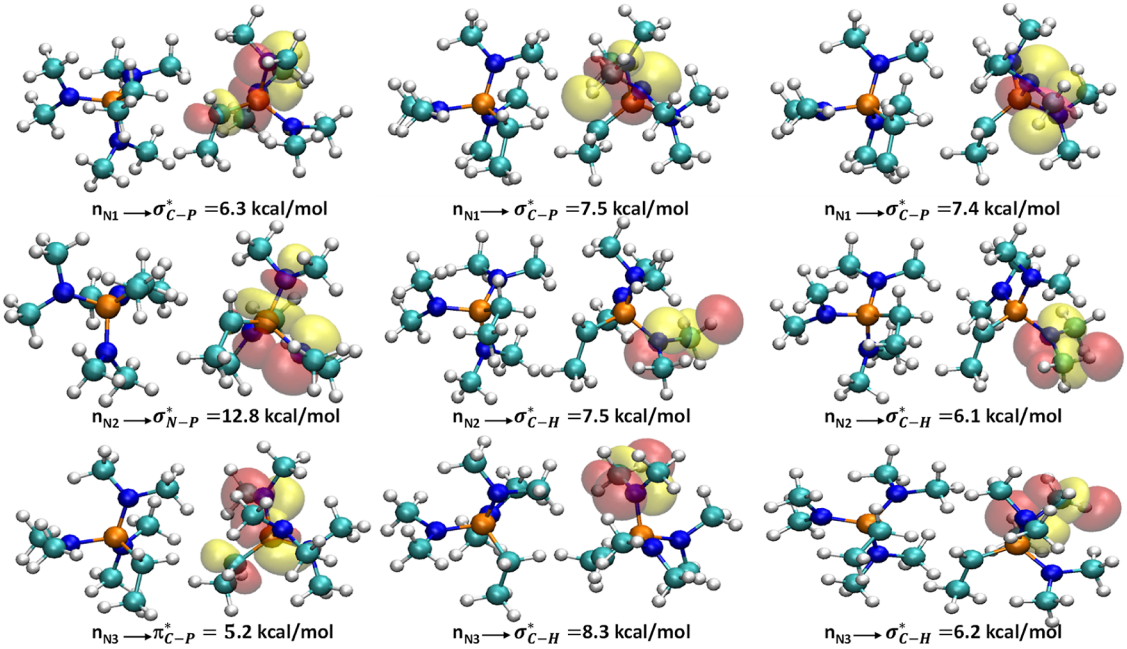

Figure 1. NBO picture of the orbital overlap of nitrogen lone pairs for the $H_2C{=}P(NMe_2)_3$ group calculated at the B3LYP-D3/6-311+G(d,p) level of theory.

positive vibrational frequency was identified, ensuring the optimized structural minimum.

The gas-phase PA value was calculated using eq 1[32]

$$PA(B) = (E_{el}) + (\Delta Z_{PVE}) \quad (1)$$

Here, $\Delta E_{el} = [E(B) - E(BH^+)]$ and $(\Delta Z_{PVE}) = [Z_{PVE}(B) - Z_{PVE}(BH^+)]$ are, respectively, the electronic and zero-point vibrational energy contributions to PA. Here, B stands for the base and BH^+ stands for the corresponding conjugate acid.

The NBO (natural bond orbital) calculation was carried out at the B3LYP-D3/6-311+G(d,p) level of theory with the NBO 3.1[33] program, implemented in Gaussian09. The second order perturbation energy E_2 was evaluated by eq 2.

$$E_2 = \Delta E_{ij} = q_i \frac{(F(i,j))^2}{\varepsilon_i - \varepsilon_j} = q_i \frac{F_{ij}^2}{\Delta\varepsilon} \quad (2)$$

where q_i is the donor orbital occupancy, ε_i and ε_j are the diagonal elements, and $F(i,j)$ is the off-diagonal NBO Fock element. A better interaction between electron donors (i) and acceptors (j) is indicated by larger E_2 values.

The wave function generated at the B3LYP-D3/6-311+G-(d,p) level using Gaussian09 was used for the Atoms-in-Molecules (AIM) analysis. Multiwfn software was used to perform AIM analysis,[34] and VMD was used for the visualization.[35]

RESULTS AND DISCUSSION

The 1,8bis(methylylidene(hexamethyltriamino)-phosphrane)naphthalene (P-MHPN) (Scheme 1 and Figure 2) consisting of two hexamethyltriaminophosphorane (P-ylide) substitutions at the 1,8-positions of naphthalene is reported as the first bisylide superbase with two interacting carbon-based basicity centers. The report reveals that the unprotonated P-ylide (**P-MHPN**) is protonated at the carbon center observed in the crystal structure and is corroborated by computational results.[22] Interestingly, the acidic proton binds with the carbon atom in the protonated P-ylide group instead of the presence of multiple nitrogen centers in the hexamethyltriaminophosphorane ($H_2C{=}P(NMe_2)_3$) group. The crystal structure of hexamethyltriaminophosphorane ($H_2C{=}P(NMe_2)_3$) has been reported in the literature.[36]

We calculated the PA value for the ($H_2C{=}P(NMe_2)_3$) group at the B3LYP-D3/6-311+G(d,p) level, and it was found to be 275.9 kcal/mol (Figure S1 and Table S1 in Supporting Information). The PA for the nitrogen analogue of the ($H_2C{=}P(NMe_2)_3$) group, i.e., ($H_2N{=}P(NMe_2)_3$) was also calculated for comparison at the same level and was found to be 261.0 kcal/mol (Figure S2 and Table S1 in Supporting Information). The result suggests that the ($H_2C{=}P(NMe_2)_3$) group has a PA value ~15.0 kcal/mol higher than that of the ($H_2N{=}P(NMe_2)_3$) group. This trend corroborates well with a previous report where the PA of ($H_2C{=}P(NMe_2)_3$) calculated at the B3LYP/6-311+G** level was 18 kcal/mol higher than that of the corresponding nitrogen analogue ($H_2N{=}P(NMe_2)_3$).[4]

To examine the more basic behavior of carbon centers in the group ($H_2C{=}P(NMe_2)_3$), we have performed conceptual DFT calculations. The Fukui function is a tool used to determine the reactivity of a molecular system by identifying the optimal location to add or remove an electron from a molecule.[37] The f^+ values describe the nucleophilicity of atoms, while f^- describes the electrophilicity of atoms.[37] The Fukui function was calculated at the B3LYP-D3/6-311+G(d,p) level for the ($H_2C{=}P(NMe_2)_3$) group. The Fukui function is defined as the change in charge for a specific atom in proportion to the change of the total number of electrons in the molecule. The Hirshfeld population analysis was used in determining the Fukui function. It is important to note that molecular sites that donate electrons are termed nucleophiles, and the basic sites of the ($H_2C{=}P(NMe_2)_3$) group must possess a higher f^+ value to capture the acidic proton.[37,38] The Fukui function values show that the carbon atom of the ($H_2C{=}P(NMe_2)_3$) group has the highest f^+ value compared to

https://doi.org/10.1021/acsomega.3c05401
ACS Omega 2023, 8, 38546−38556

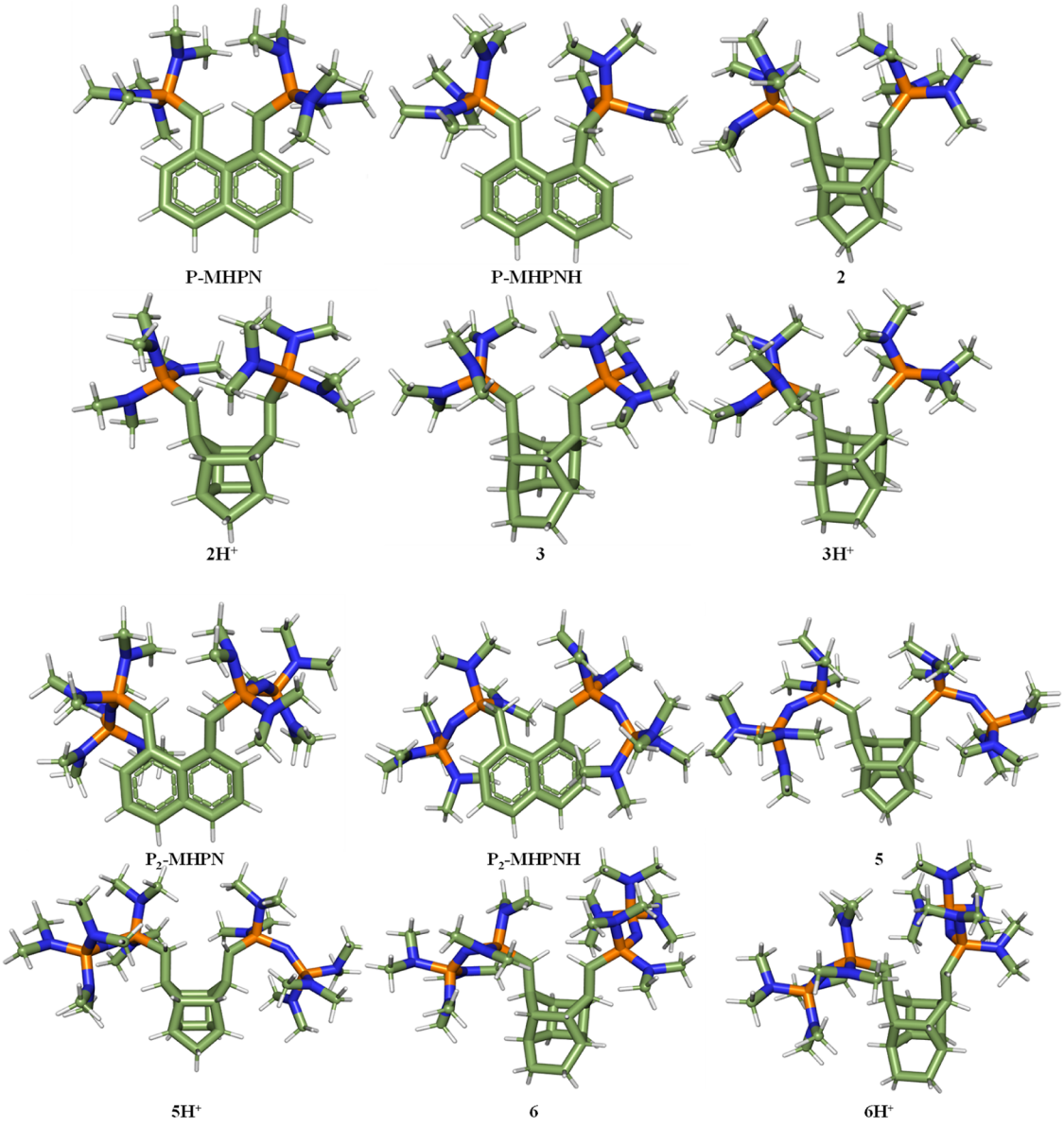

Figure 2. Optimized geometry of unprotonated and protonated superbases at the B3LYP-D3/6-311+G(d,p) level.

the nitrogen centers present in the molecule (Figure S1 and Table S2 in the Supporting Information). This finding suggests that the carbon center has higher basicity than the nitrogen centers. The lower basicity of nitrogen centers in (H_2C=$P(NMe_2)_3$) was observed with NBO analysis. The second-order perturbation energy (E_2) calculations suggest that the lone pair (n) of all three nitrogen atoms are delocalized over either the antibonding orbital (σ^*) of the corresponding C−H bonds or the antibonding orbital (σ^*) of the C−P bond. The orbital overlap visualization and its corresponding second-order perturbation energy (E_2) are shown in Figure 1. These calculated results suggest that the nitrogen lone pairs are partially engaged in the orbital interactions with neighboring bonds and hence relatively less available for interaction with the acidic proton. The PA value of bisylide was also determined using the B3LYP-D3/6-311+G(d,p) level of theory. It was observed that the PA value of bisylide was ∼8.8 kcal/mol higher than that of a single P-ylide group (Figure S3 and Table S1 in Supporting Information). Through the NBO analysis conducted on the bisylide group, it was found that there is an electron charge transfer occurring from the π_{C-P} orbital of one P-ylide group to the other σ_{C-H}* orbital of the other P-ylide group (E_2 value of 4.8 kcal/mol) (Figure S3 in Supporting Information). This electron transfer occurrence may account for the higher PA value observed for the bisylide group.

The B3LYP-D3/6-311+G(d,p) level of theory was employed to optimize the **P-MHPN** and the protonated **P-MHPNH** systems, and the optimized structures were found to be in good agreement with the corresponding crystal structures [Figure S4, and Table S3 in Supporting Information]. The naphthalene backbone of the unprotonated bisylide (**P-MHPN**) exhibits severe out-of-plane distortion of 11.3 and 12.3° in the crystal structure.[22] The values for the former mentioned plane are similar to the optimized geometry of **P-MHPN** (Table S3 serial no. 23, 24 in Supporting Information). The PA computed for **P-MHPN** at the B3LYP-D3/6-311+G(d,p) level was found to be 278.0 kcal/mol (Table 1), in good agreement with the reported PA (277.9 kcal/mol) at the M062*X*/6-311+G**//M062*X*/6-31G* level of theory.[22]

https://doi.org/10.1021/acsomega.3c05401
ACS Omega 2023, 8, 38546−38556

Table 1. Gas-Phase PAs Calculated at the B3LYP-D3/6-311+G(d,p) Level of Theory

system	PA (kcal/mol)	system	PA (kcal/mol)
P-MHPN	278.0	**P_2-MHPN**	294.6
2	283.2	**5**	303.3
3	286.5	**6**	301.0

In our study, the **P-MHPN** was optimized at M062*X*/6-31G(d) and B3LYP-D3/6-311+G(d,p) levels, which have shown similarity with the available crystal structure. The superbase calculations with a variety of systems are performed with the B3LYP DFT functional, hence this functional was used for the study.[39,40] There are several reports where B3LYP-D3 were employed in calculating PAs, and a reasonable agreement was found between the experimental and computated PA values.[41,42] The presence of an intramolecular (−C−H···C−) interaction in the protonated **P-MHPN** helps in alleviating the steric strain in the unprotonated base. This naphthalene framework, which was employed to synthesize **P-MHPN** and anchored to P-ylide to generate the superbase, is similar to a class of nitrogen-based 1,8-bis(dimethylamino)-naphthalene-type superbases, where the N−H···N hydrogen bonding plays a predominant role in achieving super-basicity.[8,9,27] Therefore, exploiting the possibility of intra-molecular −C−H···C− interaction opens a new avenue for the design of neutral organic superbases.

The hydrogen bond under investigation is often represented by the symbols D−H···A, where D stands for the donor atom and A for the acceptor atom. In the case of **P-MHPNH**, both the D and A atoms are expected to consist of just carbon centers. In the presence of any H bonding in D−H···A systems, the D−A distance would be smaller than the total van der Waals radii of D and A.[2,4,14,43] The distance between the donor C and the acceptor C in the optimized structure of **P-MHPNH** was found to be 3.0 å, which is less than the sum of their van der Waals radii (3.5 Å). However, it is now widely accepted that this H-bond criterion is excessively restrictive and only applies to strong hydrogen bonds.[1,4] It has been demonstrated that the H···A distance, in a D-H···A-type hydrogen bond is a criterion for verifying the D−H···A hydrogen bond,[16,44] and the ∠DHA is anticipated to be close to 180°.[4] In the **P-MHPNH** geometry, the H···C distance is 2.3 Å (Table 2),

Table 2. C···H Distance and ∠CHC from the Optimized Geometries of Systems (P-MHPN, P_2-MHPN, and $2H^+$−$6H^+$) Calculated at the B3LYP-D3/6-311+G(d,p) Level of Theory

system	distance C···H (Å)	∠CHC (degree)
P-MHPNH	2.3	120.7
$2H^+$	2.1	145.1
$3H^+$	1.9	149.0
P_2-MHPNH	2.3	125.8
$5H^+$	2.2	131.7
$6H^+$	2.0	143.8

which is less than the total value of van der Waals radii of individual carbon and hydrogen atoms, and ∠CHC is 120° (Table 2). The −C−H bond of one P-ylide group functions as an acceptor unit in the −C−H···C− interaction generated in **P-MHPNH**, while the π-bond of C═P of the other P-ylide group serves as the acceptor unit. The interaction of −C−H with the other P-ylide group in the **P-MHPN** system does not fall in the category of a typical −C−H/π interaction. In the case of a typical −C−H/π interaction, the orientation of the −C−H bond is supposed to align toward the interacting π-bond, and the angle range largely lies at ∼90°.[45−47] In this case, the ∠CHC for the studied systems lies in between 120° - 149°, and the −C−H bond interacts with the P-ylide group in the σ-plane of the −C═P unit. The larger population of π-electrons toward the carbon of the −C═P unit assists in interacting with the −C−H bond of another P-ylide group.[25]

Bader's theory of AIM suggests the existence of a bond critical point (BCP), and (3, −1) critical point along the bond path between the interacting atoms is an adequate condition to prove the interaction between the concerned two atoms.[4,14,48,49] Koch and Popelier also presented eight requirements, including the presence of a BCP along the bond path, for the existence of a hydrogen bond.[50] Therefore, the presence of a BCP point of **P-MHPNH** (Figure 3) between the protonated P-ylide group and the unprotonated P-ylide group signifies the −C−H···C− interaction.

In **P-MHPN**, the naphthalene ring framework anchored with bisylide was employed to achieve the basicity with the −C−H···C− interaction. It was reported that substituting the naphthalene frame with the cage polycyclic framework with nitrogen-containing groups such as amines and imines results in higher basicity than their corresponding prototype, DMAN or HMPN.[51,52] These versatile frameworks can accommodate a range of functional groups, which further enhance the basicity. Moreover, the saturated framework substantially minimizes the side reactions and is structurally robust compared with unsaturated frameworks. The flexibility of these polycyclic rings allows for a better −C−H···C− interaction than the naphthalene prototypes.[51,52] Herein, pentacyclo-[5.4.0.0.^{2,6}0.^{3,10}0^{5,9}]undecane (PCU) (**2**) with endo, endo-8,11-bisylide substitution and pentacyclo[6.4.0.0.^{2,7}0.^{3,11}0^{6,10}]-dodecane (PCD) (**3**) with endo, endo-9,12-bisylide substitution were exploited to generate superbases (Scheme 1 and Figure 2). The PA values calculated for **2** and **3** are 283.2 and 286.5 kcal/mol, respectively (Table 1). The PA of **2** is ∼5.2 kcal/mol and the PA of **3** is ∼8.5 kcal/mol higher than that of **P-MHPN** (Table 1). The literature report suggests that the higher homologue of P-ylide (P_2-ylide) anchored with naphthalene (**P_2-MHPN**) improves the basicity.[22] Therefore, the enhancement of basicity with P_2-ylide anchored to the PCU and PCD framework was studied. The gas phase PA values for **P_2-MHPN**, **5**, and **6** were calculated at the B3LYP-D3/6-311+G(d,p) level of theory (Table 1).

The reported PA for **P_2-MHPN** calculated at the M062*X*/6-311+G**//M062*X*/6-31G* level was found to be 294.7 kcal/mol and was in very good agreement with the PA value calculated at the B3LYP-D3/6-311+G(d,p) level (**P_2-MHPN** PA = 294.6 kcal/mol) (Table 1). The calculated PA for PCU with P_2-ylide (**5**) was 303.3 kcal/mol and for PCD (**6**) framework was 301.0 kcal/mol (Table 1). Interestingly, the PA values of **5** and **6** were higher than 300.0 kcal/mol, which comes in the hyperbase range (Table 1). The geometrical parameters of all the studied bases indicate a (−C−H···C−) interaction. In all the cases, the −C···H distances are shorter than the sum of their respective van der Waals radii (Table 2). In the case of **2**, **3**, **5**, and **6**, the flexible PCU and PCD frameworks allow the ∠CHC to be more alien toward 180° as compared to **P-MHPN** and **P_2-MHPN** (Table 2), favoring the possibility of a better (−C−H···C−) interaction. However, the

https://doi.org/10.1021/acsomega.3c05401
ACS Omega 2023, 8, 38546−38556

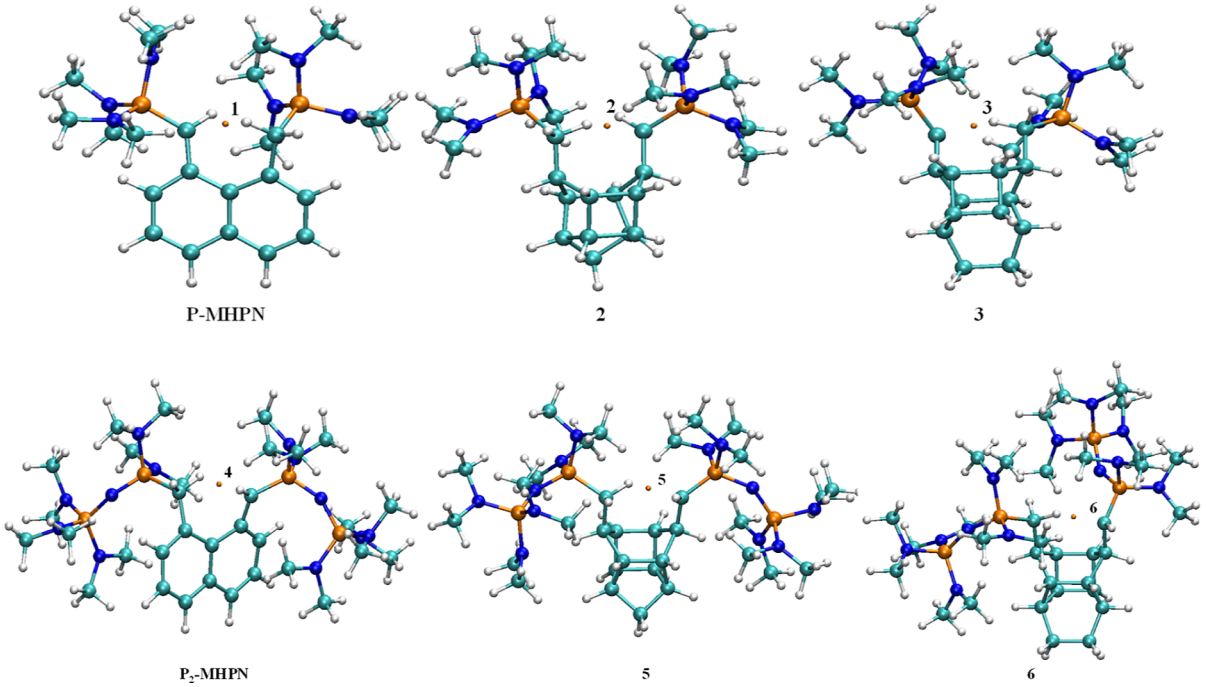

Figure 3. BCPs of **P-MHPNH-6H$^+$** calculated at the B3LYP-D3/6-311+G(d,p) level.

bulkier P_2-ylide substitutions in **5** and **6** hinder the ∠CHC and are devoid of linearity (Table 2). The AIM offers effective tools and techniques for examining the hydrogen bonding interaction, and the related parameters are well documented.[1,14,48,50,53] From the topological parameter $\nabla^2\rho$ and the total electron energy density H_C, the type of hydrogen bonding can be categorized into strong, weak, and moderate types. The weak and moderate hydrogen bonds demonstrate positive $\nabla^2\rho$ and H_C values, while for strong hydrogen bonding, the $\nabla^2\rho$ value is positive and the H_C value is negative.[1,54] The BCPs and positive $\nabla^2\rho$ values indicate a closed-shell interaction in all cases (Figure 3, Table 3).

Table 3. Topological Parameters of the −C−H···C− Interacting Systems Calculated at the B3LYP-D3/6-311+G(d,p) Level; Topological Parameters Are in au

system	V (r)	G (r)	H (r)	$\nabla^2\rho_{C\cdots H}$	$\rho_{C\cdots H}$
P-MHPNH	−0.012	0.014	0.0019	0.063	0.020
2H$^+$	−0.018	0.018	−0.0002	0.071	0.028
3H$^+$	−0.029	0.023	−0.0056	0.069	0.041
P_2-MHPNH	−0.013	0.016	0.0029	0.076	0.021
5H$^+$	−0.013	0.014	0.0005	0.057	0.023
6H$^+$	−0.021	0.019	−0.0024	0.065	0.034

Analyzing the topological parameters $\nabla^2\rho$ and H_C, it was concluded that in the case of **P-MHPNH**, both the $\nabla^2\rho_{C\cdots H}$ and H_C values are positive, indicating the possibility of a weak or moderate (−C−H···C−) interaction. However, in the case of **2H$^+$** and **3H$^+$**, the positive $\nabla^2\rho$ values and negative H_C values indicate the possibility of a strong (−C−H···C−) interaction. These parameters also suggest weak or moderate (−C−H···C−) interactions for **P_2-MHPNH** and **5H$^+$** and a stronger interaction for **6H$^+$**.

One of the key features associated with any interaction and specifically hydrogen bonding is the electron charge transfer from the lone pair of the donor (n_B) to the empty antibonding orbital of the acceptor (σ_{AH^*}).[48] In all the studied bases, charge transfer of $\pi_{C-P} \rightarrow \sigma_{C-H}^*$ was observed, where the π_{C-P} bond of one of the P-ylide groups acts as the donor and the σ_{C-H}^* of the other P-ylide group acts as the acceptor. The NBO analysis of P-ylide-substituted bases reveals that the E_2 energy value increases progressively from **P-MHPNH** to **2H$^+$** and **3H$^+$** (Table 4). The highest E_2 energy value observed with **3H$^+$**

Table 4. $\pi_{C-P} \rightarrow \sigma_{C-H}^*$ Interaction of the Bases Calculated at the B3LYP-D3/6-311+G(d,p) Level of Theory

system	E_2 (kcal/mol)	system	E_2 (kcal/mol)
P-MHPNH	2.5	**P_2-MHPNH**	2.2
2H$^+$	8.2	**5H$^+$**	6.4
3H$^+$	20.5	**6H$^+$**	15.1

(E_2 = 20.5 kcal/mol) indicates the greatest $\pi_{C-P} \rightarrow \sigma_{C-H}^*$ charge transfer from the π_{C-P} donor to the σ_{C-H}^* acceptor (Table 4). Importantly, this E_2 energy of $\pi_{C-P} \rightarrow \sigma_{C-H}^*$ electron donation closely relates to the ∠CHC. As the ∠CHC reaches better linearity from **P-MHPNH** to **2H$^+$** and **3H$^+$**, the $\pi_{C-P} \rightarrow \sigma_{C-H}^*$ donation increases, resulting in a higher E_2 energy value (Table 2, Table 4). A similar trend was also observed for P_2-ylide, where the E_2 energy value of the $\pi_{C-P} \rightarrow \sigma_{C-H}^*$ electron increases from **P_2-MHPNH** to **5H$^+$** and **6H$^+$** (Table 4), indicating improved donation. However, the E_2 energy values for the conjugate acid of the P_2-ylide bases are lower than those for the conjugate acid of the P-ylide bases (Table 4). The bulkier P_2-ylide substitutions hinder the ∠CHC of the corresponding conjugate acids to achieve linearity, resulting in lower E_2 energy values.

Several experimental and theoretical studies have provided insights into the nature of hydrogen bonds in the protonated form of nitrogen-containing superbases. These studies indicate that hydrogen bonds can be either symmetric or asymmetric.[55] In the case of asymmetric hydrogen bonds, the hydrogen atom exists in a double well potential, while in the case of symmetric

https://doi.org/10.1021/acsomega.3c05401
ACS Omega 2023, 8, 38546−38556

hydrogen bonds, it resides in a single well potential.[55,56] The NMR study conducted on the protonated form of 1,8-bis(dimethylamino)naphthalene revealed the asymmetric nature of the −N−H−N− bond, and the proton resides in the double minimum potential forming rapid interconvertible tautomers.[56] Similarly, the NMR study on the protonated form of HMPN, which is the nitrogen analogue of **P-MHPN**, demonstrated the presence of an unsymmetrical hydrogen bond with fast intramolecular proton exchange between the two nitrogen atoms.[27] In the case of **P-MHPNH**, the NMR study shows the protonated form of **P-MHPNH** which undergoes a rapid intramolecular proton exchange between the carbon atoms of both the ylide groups.[22] The activation free-energy barrier for this proton exchange process calculated in the gas phase at the M062*X*/6-311+G**//M062*X*/6-31G* level was found to be 14.5 kcal/mol.[22] This value is relatively higher than the free activation energy of the corresponding nitrogen analogue, HMPN. The reported value for the free energy of activation calculated at the M062*X*/6-311+G**//M062*X*/6-31G* level was in good agreement with the experimentally calculated free activation energy value (12.9 kcal/mol). Therefore, the M062*X*/6-31G* level was employed to recalculate the free energy of activation for the studied systems. The free energy of activation value recalculated for **P-MHPNH** was 15.2 kcal/mol, which was in good agreement with the reported value. In the case of $\mathbf{2H^+}$ and $\mathbf{3H^+}$, the values were found to be 1.9 and 6.4 kcal/mol, respectively (Table S5 in Supporting Information). However, the free energy of activation value for **P-MHPNH** was substantially higher than those of $\mathbf{2H^+}$ and $\mathbf{3H^+}$. The results obtained from calculations involving van der Waals radii, AIM, and NBO align closely with the values documented in the literature for the identification of hydrogen bonds, supporting the presence of similar types of hydrogen bonding interactions in bisylide systems. Therefore, the result suggests a possible neutral (−C−H···C−)-type hydrogen bonding interaction in the designed P-ylide-substituted bases.

To unravel the factors that influence the basicity of the studied molecules, isodesmic calculations were performed for all the bases (**P-MHPN** to **6**) (Figure 4, Table 5).[57] The strain energies of the unprotonated bases were calculated from the isodesmic setups (Figure 4, Table 5) using optimized geometries of the corresponding systems at the B3LYP-D3/6-311+G(d,p) level. The geometry of X mentioned in Figure 4 suffers from severe steric stain due to the close proximity of two bulky P-ylide substitutions in the unprotonated systems. To estimate the strain energy present in the unprotonated systems, one of the bulky P-ylide substitutions was replaced with a hydrogen atom (Figure 4, X_b) minimizing the steric strain. The calculated strain energy is mentioned in the first column of Table 5.

The peri-strain generated due to the substitutions at the 1,8 positions of naphthalene is the highest for **P-MHPN** and **P_2-MHPN**. The flexible PCU and PCD scaffolds with P-ylide substitution generate relatively less strain in the case of superbases **2** and **3**. It is to be noted that as the strain in the unprotonated cage scaffold decreases, ∠CHC becomes more linear, resulting in a better (−C−H···C−) interaction. However, in the case of **5** and **6**, the strain energy is much higher (Table 5) due to the bulkier P_2-ylide substituents, which also affect the linearity of ∠CHC and the (−C−H···C−) interaction.

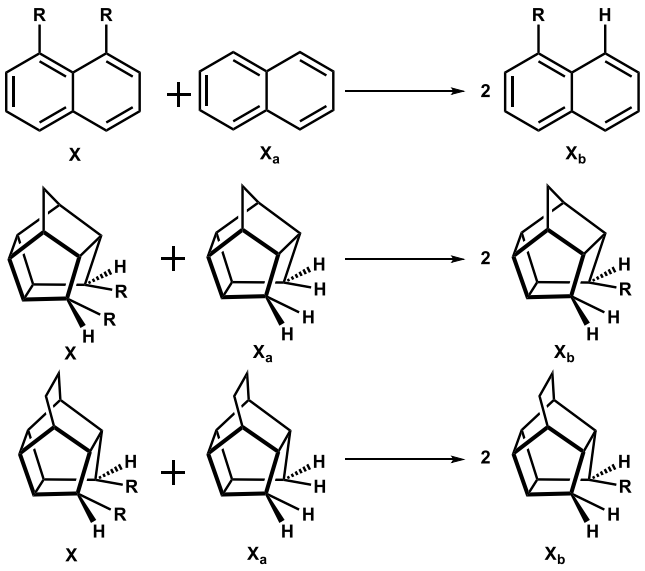

Figure 4. Isodesmic setups to calculate strain energies for unprotonated compounds **P-MHPN**, **P_2-MHPN**, and **2**−**6**. The $SE(X) = E(X) + E(X_a) - 2E(X_b)$ equation is employed to calculate the strain energy. Here, R═P-ylide for **P-MHPN**, **2**, **3**, and R═P_2-ylide for **P_2-MHPN**, **5**, and **6**.

Table 5. Strain Energies (SE), Strain Energies + Interaction Energies $(SE + IE)^+$, and Interaction Energies (IE) Calculated at the B3LYP-D3/6-311+G(d,p) Level for Conjugate Acids[a]

system	strain energy (SE) (kcal/mol)	strain + (−C−H···C−) interaction energy energies $(SE + IE)^+$(kcal/mol)	(−C−H···C−) interaction energy (IE) (kcal/mol)
P-MHPN	7.4	−2.0	−14.8
2	1.7	−3.5	−12.2
3	0.7	−6.8	−16.5
P_2-MHPN	7.1	−7.1	−12.5
5	4.4	−6.9	−13.2
6	4.7	−6.6	−20.8

[a]The values are in kcal/mol.

In the protonated bases, the steric strain is relieved due to the formation of an intramolecular (−C−H···C−) interaction in the unprotonated bases. An isodesmic setup was prepared to estimate the stabilizing effect of SE and $(SE + IE)^+$ (Figure 5 and Table 5).[57] These isodesmic reactions offer a qualitative estimation of intramolecular interactions and should not be employed for quantitative purposes. The geometry mentioned in the isodesmic reaction in Figure 5 was optimized at the B3LYP-D3/6-311+G(d,p) level of theory. In the geometry XH^+ (Figure 5), the stabilizing (−C−H···C−) interaction lowered the steric strain. In X^a (Figure 5), the protonated P-ylide group was kept constant, whereas the other bulky P-ylide substitution was replaced with hydrogen to eliminate the steric strain. The other terms present in the isodesmic setup (Figure 5) were incorporated to satisfy the isodesmic equation. The $(SE + IE)^+$ energies are provided in the second column of Table 5. The negative sign of $(SE + IE)^+$ energies indicates after protonation the conjugate acid achieves an overall stabilization compared to unprotonated bases. In P-ylide substitution, the $(SE + IE)^+$ increase progressively from **P-MHPN** to **3**, indicating the stabilization of the corresponding

https://doi.org/10.1021/acsomega.3c05401
ACS Omega 2023, 8, 38546−38556

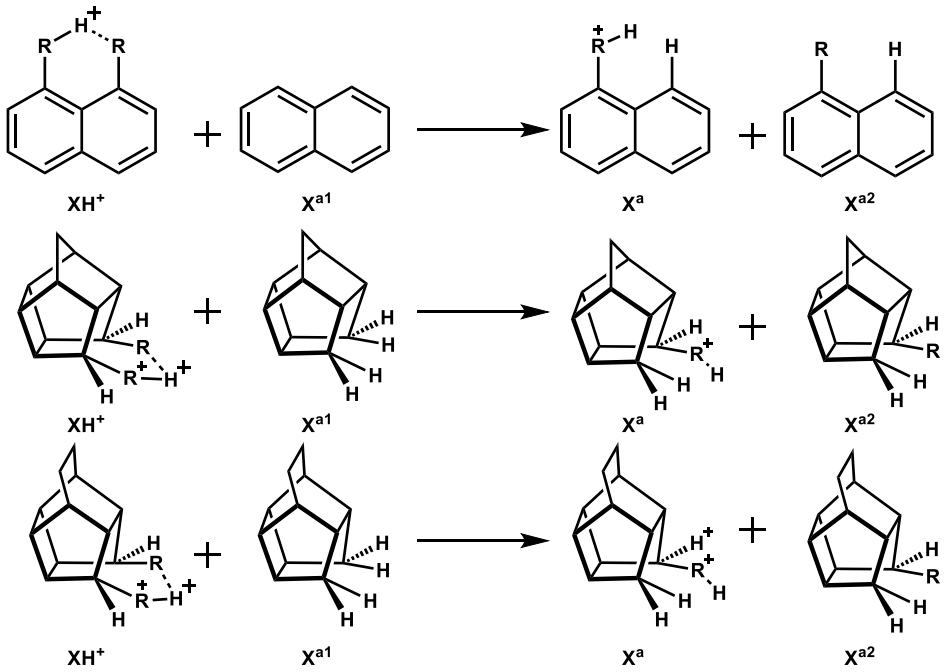

Figure 5. Isodesmic setups to calculate the sum of cation strain energies (SE) and (−C−H···C−) interaction energies (SE + IE)$^+$, for **P-MHPN**, **P$_2$-MHPN**, and **2**−**6**. The {[IE(XH$^+$) + SE(XH$^+$)] = E(XH$^+$) + E(X^{a1}) − E(X^a) − E(X^{a2})} equation is employed to calculate cumulative (SE + IE)$^+$, where R═P-ylide is for **P-MHPN**, **2**, and **3**, and R═P$_2$-ylide is for **P$_2$-MHPN**, **5**, and **6**.

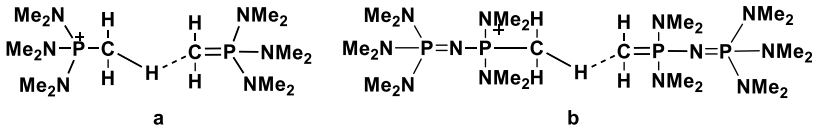

Figure 6. Model systems used to estimate cationic hydrogen bond energies for (a) **P-MHPNH**, **2H**$^+$, and **3H**$^+$ and (b) **P$_2$-MHPNH**, **4H**$^+$, and **5H**$^+$.

conjugate acids (Figure 5 and Table 5). System **3** shows the highest (SE + IE)$^+$ stabilization energy of −6.8 kcal/mol and the lowest SE, resulting in the highest PA value for P-ylide substituents. However, in the case of P$_2$-ylide, the (SE + IE)$^+$ stabilization energies for **P$_2$-MHPN**, **5**, and **6** are comparable. In the case of P$_2$-ylide, the bulkiness of the substituents hinders the cumulative cationic and (−C−H···C−) stabilization for the studied systems.

To estimate the (−C−H···C−) interaction from the (SE + IE)$^+$ stabilizations, an independent model study was performed (Figure 6 and Table 5). In the model systems, only the proton-bound bisylide was separated from the respective main scaffold, and the valences were satisfied by adding hydrogen atoms. Single-point calculations (vibrationless) were performed with the respective geometries at the B3LYP-D3/6-311+G(d,p) level, and the individual molecules were separated at an infinite distance to evaluate the respective energies.[57] These calculations yielded (−C−H···C−) interaction energies in the range of approximately 12.5 to 20.8 kcal/mol, which are comparatively higher than the strain energy calculated for the unprotonated bases (Table 5). In the case of P-ylide substitution, **3** shows the highest (−C−H···C−) interaction energy. The lower strain in **3** allows the system to form a better (−C−H···C−) interaction. The augmented basicity of P-ylide-substituted **3** results from the cumulative effect of a lower strain of the unprotonated scaffolds, greater (SE + IE)$^+$ stabilization, and a higher IE interaction. In the case of P$_2$-ylide substitution, system **6** with PCD scaffold possesses the highest (−C−H···C−) interaction energy, followed by system **5** with the PCU scaffold, followed by **P$_2$-MHPN** (Table 5). The hyperbase **6** possesses the highest interaction energy (IE); however, the bulkier P$_2$-ylide substitution diminishes the (SE + IE)$^+$ energy lowering the PA of **6** to that of system **5**. The isodesmic results suggest that the basicity appears to represent the combined effect of the relative cation strain generated upon protonation, the induced strain by the bulky ylide substitutions, and the establishment of a strong intramolecular (−C−H···C−) interaction in protonated systems.

Under experimental conditions for organic superbases, acetonitrile is employed as the solvent medium. Therefore, PAs for all the designed bases were calculated in acetonitrile solvent (ε = 36.64) at the B3LYP-D3/6-311G+(d,p) level using the CPCM (conductor-like polarizable continuum) solvent model (Table 6). Notably, the PA values calculated in the solvent phase for all the designed systems exceeded 300.0 kcal/mol and can function as hyperbases in the solvent medium.

Table 6. Calculated PA Values in Acetonitrile Solvent Calculated at the B3LYP-D3/6-311+G(d,p) Level of Theory

system	PA (kcal/mol)	system	PA (kcal/mol)
P-MHPN	314.0	**P$_2$-MHPN**	321.3
2	323.5	**5**	335.4
3	224.9	**6**	333.8

https://doi.org/10.1021/acsomega.3c05401
ACS Omega 2023, 8, 38546−38556

CONCLUSIONS

In this study, we have exploited a (−C−H···C−) interaction-functionalized cage framework with a bisylide group to design organic superbases. Recently, an experimental report reveals the organic superbase with bisylide substitution in the naphthalene unit (**P-MHPN**). This compound demonstrates a much higher basicity when compared to its nitrogen analogue (HMPN). The enhanced basicity of HMPN is attributed to the contribution of −N−H···N- hydrogen bonding, whereas the −C−H···C− interaction contributes in enhancing the basicity of **P-MHPN**. We have explored the bisylide group with pentacyclo[5.4.0.0.2,60.3,100^{5,9}]undecane (PCU) and pentacyclo [6.4.0.0.2,70.3,1106,10] dodecane (PCD) scaffolds in designing superbases and hyperbases using the B3LYP-D3/6-311+G(d,p) level of theory. The bisylide group exhibits two interacting carbon-based basicity centers. The computational results suggest that the nitrogen lone pairs of the P-ylide group are partially engaged in the orbital interactions with neighboring σ_{C-H}* and σ_{C-P}* bonds and hence make the carbon center more basic in the bisylide group. The predicted PAs for these polycyclic cage compounds were found to be higher than those of the corresponding prototypes, **P-MHPN** and **P$_2$-MHPN**. The calculated basicities are in the range of hyperbase in acetonitrile medium. The flexibility of these PCU and PCD scaffolds allows ∠CHC of the bisylide groups to be more alien toward linearity, resulting in a better −C−H···C− interaction. Consequently, this improved −C−H···C− interaction favors the enhancement of the PA of the bases. In the −C−H···C- bridged interaction, the π-bond, largely localized over the carbon atom of one of the P-ylides, interacts with the σ_{C-H}* orbital of the other P-ylide group. Comparing the literature reported values for the hydrogen bonding interaction with the calculated results suggests a possible neutral −C−H···C− hydrogen bonding interaction in the P-ylide bases. The higher analogue of P-ylide (P$_2$-ylide) substituted with PCU and PCD scaffolds results in hyperbases. The improved basicity of P-ylide groups seems to be the cumulative effect of strain relative to the conjugate acids and the establishment of −C−H···C− interaction in the protonated systems.

ASSOCIATED CONTENT

Supporting Information

The Supporting Information is available free of charge at https://pubs.acs.org/doi/10.1021/acsomega.3c05401.

Optimized geometries, calculated PA values, calculated Fukui functions for C and N atoms, comparison of bond lengths and bond angles, topological parameters, calculated free activation energy of proton exchange, and coordinates of the studied systems (PDF)

AUTHOR INFORMATION

Corresponding Author

Bishwajit Ganguly − *Computation and Simulation Unit, Analytical and Environmental Science Division and Centralized Instrument Facility, CSIR-Central Salt & Marine Chemicals Research Institute, Bhavnagar, Gujarat 364002, India; Academy of Scientific and Innovative Research (AcSIR), Ghaziabad 201002, India;* orcid.org/0000-0001-9682-7456; Email: gang_12@rediffmail.com, ganguly@csmcri.res.in; Fax: (+91)-278-2567562

Author

Anusuya Saha − *Computation and Simulation Unit, Analytical and Environmental Science Division and Centralized Instrument Facility, CSIR-Central Salt & Marine Chemicals Research Institute, Bhavnagar, Gujarat 364002, India; Academy of Scientific and Innovative Research (AcSIR), Ghaziabad 201002, India*

Complete contact information is available at: https://pubs.acs.org/10.1021/acsomega.3c05401

Notes

The authors declare no competing financial interest.

ACKNOWLEDGMENTS

A.S. acknowledges Academy of Scientific & Innovative Research (AcSIR), Ghaziabad, Uttar Pradesh-201002, India, for enrollment in the PhD program. A.S. thanks Dr. Rabindranath Lo and Dr. Sukalyan Bhadra for all their favors. CSIR-CSMCRI registration number: PRIS-no: 97/2023. We are thankful to the reviewers for their valuable comments and suggestions that have helped us to improve the paper.

REFERENCES

(1) Grabowski, S. J. What Is the Covalency of Hydrogen Bonding? *Chem. Rev.* **2011**, *111* (4), 2597−2625.

(2) Pauling, L.; Wheland, G. W. The Nature of the Chemical Bond. V. *J. Chem. Phys.* **1934**, *2* (8), 482.

(3) Koppel, I. A.; Schwesinger, R.; Breuer, T.; Burk, P.; Herodes, K.; Koppel, I.; Leito, I.; Mishima, M. Intrinsic Basicities of Phosphorus Imines and Ylides: A Theoretical Study. *J. Phys. Chem. A* **2001**, *105* (41), 9575−9586.

(4) Raghavendra, B.; Arunan, E. Unpaired and σ Bond Electrons as H, Cl, and Li Bond Acceptors: An Anomalous One-Electron Blue-Shifting Chlorine Bond. *J. Phys. Chem. A* **2007**, *111* (39), 9699−9706.

(5) Panich, A. M. NMR Study of the F-H···F Hydrogen Bond. Relation between Hydrogen Atom Position and F-H···F Bond Length. *Chem. Phys.* **1995**, *196* (3), 511−519.

(6) Kawabata, T.; Jiang, C.; Hayashi, K.; Tsubaki, K.; Yoshimura, T.; Majumdar, S.; Sasamori, T.; Tokitoh, N. Axially Chiral Binaphthyl Surrogates with an Inner N-H-N Hydrogen Bond. *J. Am. Chem. Soc.* **2009**, *131* (1), 54−55.

(7) Deepak, R. N. V. K.; Sankararamakrishnan, R. Unconventional N-H···N Hydrogen Bonds Involving Proline Backbone Nitrogen in Protein Structures. *Biophys. J.* **2016**, *110* (9), 1967−1979.

(8) Raab, V.; Kipke, J.; Gschwind, R. M.; Sundermeyer, J. 1,8-Bis(Tetramethylguanidino)Naphthalene (TMGN): A New, Superbasic and Kinetically Active "Proton Sponge. *Chem.—Eur. J.* **2002**, *8* (7), 1682−1693.

(9) Alder, R. W.; Bowman, P. S.; Steele, W. R. S.; Winterman, D. R. The Remarkable Basicity of 1,8-Bis(Dimethylamino)Naphthalene. *Chem. Commun.* **1968**, *13*, 723.

(10) Parthasarathi, R.; Subramanian, V.; Sathyamurthy, N. Hydrogen Bonding without Borders: An Atoms-in-Molecules Perspective. *J. Phys. Chem. A* **2006**, *110* (10), 3349−3351.

(11) Alkorta, I.; Rozas, I.; Elguero, J. Non-Conventional Hydrogen Bonds. *Chem. Soc. Rev.* **1998**, *27* (2), 163.

(12) Grabowski, S. J. Ab Initio Calculations on Conventional and Unconventional Hydrogen BondsStudy of the Hydrogen Bond Strength. *J. Phys. Chem. A* **2001**, *105* (47), 10739−10746.

(13) Dutta, J.; Sahu, A. K.; Bhadauria, A. S.; Biswal, H. S. Carbon-Centered Hydrogen Bonds in Proteins. *J. Chem. Inf. Model.* **2022**, *62* (8), 1998−2008.

(14) Chandra, A. K.; Zeegers-Huyskens, T. Theoretical Study of (CH···C) - Hydrogen Bonds in CH 4- n X n (X = F, Cl; n = 0, 1, 2) Systems Complexed with Their Homoconjugate and Heteroconjugate Carbanions. *J. Phys. Chem. A* **2005**, *109* (51), 12006−12013.

(15) Platts, J. A.; Howard, S. T.; Woźniak, K. Quantum Chemical Evidence for C-H ··· C Hydrogen Bonding. *Chem. Commun.* **1996**, *1*, 63−64.
(16) Klein, R. A. Modified van Der Waals Atomic Radii for Hydrogen Bonding Based on Electron Density Topology. *Chem. Phys. Lett.* **2006**, *425* (1−3), 128−133.
(17) Arunan, E. One Hundred Years After the Latimer and Rodebush Paper, Hydrogen Bonding Remains an Elephant! *J. Indian Inst. Sci.* **2020**, *100* (1), 249−255.
(18) Webber, A. L.; Yates, J. R.; Zilka, M.; Sturniolo, S.; Uldry, A.-C.; Corlett, E. K.; Pickard, C. J.; Pérez-Torralba, M.; Angeles Garcia, M.; Santa Maria, D.; Claramunt, R. M.; Brown, S. P. Weak Intermolecular CH···N Hydrogen Bonding: Determination of 13 CH- 15 N Hydrogen-Bond Mediated J Couplings by Solid-State NMR Spectroscopy and First-Principles Calculations. *J. Phys. Chem. A* **2020**, *124* (3), 560−572.
(19) Gautam, S. T. D. *The Weak Hydrogen Bond in Structural Chemistry and Biology, Oxford University Press/International Union of Crystallography, Oxford*; Oxford University Press, 1999.
(20) Isaev, A. N. C-H···O, O-H···C, and C-H···C Interactions in Complexes of Carbocations and Carboanions. *Russ. J. Inorg. Chem.* **2013**, *58* (7), 817−823.
(21) Ishikawa, T. *Superbases for Organic Synthesis: Guanidines, Amidines, Phosphazenes and Related Organocatalysts*; John Wiley & Sons, Ltd, 2009..
(22) Kögel, J. F.; Margetić, D.; Xie, X.; Finger, L. H.; Sundermeyer, J. A Phosphorus Bisylide: Exploring a New Class of Superbases with Two Interacting Carbon Atoms as Basicity Centers. *Angew. Chem., Int. Ed.* **2017**, *56* (11), 3090−3093.
(23) Leito, I.; Koppel, I. A.; Koppel, I.; Kaupmees, K.; Tshepelevitsh, S.; Saame, J. Basicity Limits of Neutral Organic Superbases. *Angew. Chem., Int. Ed.* **2015**, *54* (32), 9262−9265.
(24) Saame, J.; Rodima, T.; Tshepelevitsh, S.; Kütt, A.; Kaljurand, I.; Haljasorg, T.; Koppel, I. A.; Leito, I. Experimental Basicities of Superbasic Phosphonium Ylides and Phosphazenes. *J. Org. Chem.* **2016**, *81* (17), 7349−7361.
(25) Kárpáti, T.; Veszprémi, T.; Thirupathi, N.; Liu, X.; Wang, Z.; Ellern, A.; Nyulászi, L.; Verkade, J. G. Synthesis and Photoelectron Spectroscopic Studies of N(CH 2 CH 2 NMe) 3 PE (E = O, S, NH, CH 2). *J. Am. Chem. Soc.* **2006**, *128* (5), 1500−1512.
(26) Kisanga, P. B.; Verkade, J. G.; Schwesinger, R. P K a Measurements of P(RNCH 2 CH 3) 3 N. *J. Org. Chem.* **2000**, *65* (17), 5431−5432.
(27) Raab, V.; Gauchenova, E.; Merkoulov, A.; Harms, K.; Sundermeyer, J.; Kovačević, B.; Maksić, Z. B. 1,8-Bis-(Hexamethyltriaminophosphazenyl)Naphthalene, HMPN: A Super-basic Bisphosphazene "Proton Sponge. *J. Am. Chem. Soc.* **2005**, *127* (45), 15738−15743.
(28) Becke, A. D. Density-functional Thermochemistry. III. The Role of Exact Exchange. *J. Chem. Phys.* **1993**, *98* (7), 5648−5652.
(29) Grimme, S.; Antony, J.; Ehrlich, S.; Krieg, H. A Consistent and Accurate Ab Initio Parametrization of Density Functional Dispersion Correction (DFT-D) for the 94 Elements H-Pu. *J. Chem. Phys.* **2010**, *132* (15), 154104.
(30) McLean, A. D.; Chandler, G. S. Contracted Gaussian Basis Sets for Molecular Calculations. I. Second Row Atoms, Z = 11−18. *J. Chem. Phys.* **1980**, *72* (10), 5639−5648.
(31) Frisch, M. J.; Trucks, G. W.; Schlegel, H. B.; Scuseria, G. E.; Robb, M. A.; Cheeseman, J. R.; Scalmani, G.; Barone, V.; Mennucci, B.; Petersson, G. A.; Nakatsuji, H.; Caricato, M.; Li, X.; Hratchian, H. P.; Izmaylov, A. F.; Bloino, J.; Zheng, G.; Sonnenberg, J. L.; Hada, M.; Ehara, M.; Toyota, K.; Fukuda, R.; Hasegawa, J.; Ishida, M.; Nakajima, T.; Honda, Y.; Kitao, O.; Nakai, H.; Vreven, T.; Montgomery, J. A., Jr.; Peralta, J. E.; Ogliaro, F.; Bearpark, M.; Heyd, J. J.; Brothers, E.; Kudin, K. N.; Staroverov, V. N.; Kobayashi, R.; Normand, J.; Raghavachari, K.; Rendell, A.; Burant, J. C.; Iyengar, S. S.; Tomasi, J.; Cossi, M.; Rega, N.; Millam, J. M.; Klene, M.; Knox, J. E.; Cross, J. B.; Bakken, V.; Adamo, C.; Jaramillo, J.; Gomperts, R.; Stratmann, R. E.; Yazyev, O.; Austin, A. J.; Cammi, R.; Pomelli, C.; Ochterski, J. W.; Martin, R. L.; Morokuma, K.; Zakrzewski, V. G.; Voth, G. A.; Salvador, P.; Dannenberg, J. J.; Dapprich, S.; Daniels, A. D.; Farkas, O.; Foresman, J. B.; Ortiz, J. V.; Cioslowski, J.; Fox, D. J. *Gaussian 09*, revision D.01; Gaussian, Inc.: Wallingford, CT, 2013.
(32) Lo, R.; Singh, A.; Kesharwani, M. K.; Ganguly, B. Rational Design of a New Class of Polycyclic Organic Bases Bearing Two Superbasic Sites and Their Applications in the CO2 Capture and Activation Process. *Chem. Commun.* **2012**, *48* (47), 5865−5867.
(33) Glendening, E. D.; Reed, A. E.; Carpenter, J. E.; Wnbo, F. *TCI*; University of Wisconsin: Madison, 1998.
(34) Lu, T.; Chen, F. Multiwfn: A Multifunctional Wavefunction Analyzer. *J. Comput. Chem.* **2012**, *33* (5), 580−592.
(35) Humphrey, W.; Dalke, A.; Schulten, K. VMD: Visual Molecular Dynamics. *J. Mol. Graphics* **1996**, *14* (1), 33−38.
(36) Mitzel, N. W.; Smart, B. A.; Dreihäupl, K. H.; Rankin, D. W. H.; Schmidbaur, H. Low Symmetry in P(NR 2) 3 Skeletons and Related Fragments: An Inherent Phenomenon. *J. Am. Chem. Soc.* **1996**, *118* (50), 12673−12682.
(37) Pucci, R.; Angilella, G. G. N. Density Functional Theory, Chemical Reactivity, and the Fukui Functions. *Found. Chem.* **2022**, *24* (1), 59−71.
(38) Yang, W.; Parr, R. G.; Pucci, R. Electron Density, Kohn-Sham Frontier Orbitals, and Fukui Functions. *J. Chem. Phys.* **1984**, *81* (6), 2862−2863.
(39) Biswas, A. K.; Ganguly, B. Revealing Germylene Compounds to Attain Superbasicity with Sigma Donor Substituents: A Density Functional Theory Study. *Chem. - Eur. J.* **2017**, *23* (11), 2700−2705.
(40) Grimme, S.; Antony, J.; Ehrlich, S.; Krieg, H. A Consistent and Accurate Ab Initio Parametrization of Density Functional Dispersion Correction (DFT-D) for the 94 Elements H-Pu. *J. Chem. Phys.* **2010**, *132* (15), 154104.
(41) Zhang, L.; Ding, X.; Kratka, C. R.; Levine, A.; Lee, J. K. Gas Phase Experimental and Computational Studies of AlkB Substrates: Intrinsic Properties and Biological Implications. *J. Org. Chem.* **2023**, *88*, 13115−13124.
(42) Váňa, J.; Roithová, J.; Kotora, M.; Beran, P.; Rulíšek, L.; Kočovský, P. Proton Affinities of Organocatalysts Derived from Pyridine N-Oxide. *Croat. Chem. Acta* **2014**, *87* (4), 349−356.
(43) Desiraju, G. R. The C-H.Cntdot.Cntdot.Cntdot.O Hydrogen Bond in Crystals: What Is It? *Acc. Chem. Res.* **1991**, *24* (10), 290−296.
(44) Lakshmi, B.; Samuelson, A. G.; Jovan Jose, K. V.; Gadre, S. R.; Arunan, E. Is There a Hydrogen Bond Radius? Evidence from Microwave Spectroscopy, Neutron Scattering and X-Ray Diffraction Results. *New J. Chem.* **2005**, *29* (2), 371.
(45) Zheng, X.; Alsalloum, A. Y.; Hou, Y.; Sargent, E. H.; Bakr, O. M. All-Perovskite Tandem Solar Cells: A Roadmap to Uniting High Efficiency with High Stability. *Acc. Mater. Res.* **2020**, *1* (1), 63−76.
(46) Umezawa, Y.; Tsuboyama, S.; Honda, K.; Uzawa, J.; Nishio, M. CH/ π Interaction in the Crystal Structure of Organic Compounds. A Database Study. *Bull. Chem. Soc. Jpn.* **1998**, *71* (5), 1207−1213.
(47) Tsuzuki, S.; Fujii, A. Nature and Physical Origin of CH/π Interaction: Significant Difference from Conventional Hydrogen Bonds. *Phys. Chem. Chem. Phys.* **2008**, *10* (19), 2584.
(48) Grabowski, S. J.; Sokalski, W. A.; Leszczynski, J. Nature of X-H $^{+\delta}$ ··· $^{-\delta}$ H-Y Dihydrogen Bonds and X-H···σ Interactions. *J. Phys. Chem. A* **2004**, *108* (27), 5823−5830.
(49) Kumar, P. S. V.; Raghavendra, V.; Subramanian, V. Bader's Theory of Atoms in Molecules (AIM) and Its Applications to Chemical Bonding. *J. Chem. Sci.* **2016**, *128* (10), 1527−1536.
(50) Koch, U.; Popelier, P. L. A. Characterization of C-H-O Hydrogen Bonds on the Basis of the Charge Density. *J. Phys. Chem.* **1995**, *99* (24), 9747−9754.
(51) Singh, A.; Ganguly, B. DFT Studies on a New Class of Cage Functionalized Organic Superbases. *New J. Chem.* **2009**, *33* (3), 583−587.
(52) Singh, A.; Ganguly, B. DFT Studies toward the Design and Discovery of a Versatile Cage-Functionalized Proton Sponge. *Eur. J. Org Chem.* **2007**, *2007* (3), 420−422.

https://doi.org/10.1021/acsomega.3c05401
ACS Omega 2023, 8, 38546−38556

(53) Bader, R. F. W. Atoms in Molecules. *Acc. Chem. Res.* **1985**, *18* (1), 9−15.
(54) Rozas, I.; Alkorta, I.; Elguero, J. Behavior of Ylides Containing N, O, and C Atoms as Hydrogen Bond Acceptors. *J. Am. Chem. Soc.* **2000**, *122* (45), 11154−11161.
(55) Frey, P. A.; Cleland, W. W. Are There Strong Hydrogen Bonds in Aqueous Solutions? *Bioorg. Chem.* **1998**, *26* (4), 175−192.
(56) Perrin, C. L.; Ohta, B. K. Symmetry of N-H-N Hydrogen Bonds in 1,8-Bis(Dimethylamino)Naphthalene·H + and 2,7-Dimethoxy-1,8-Bis(Dimethylamino)Naphthalene·H +. *J. Am. Chem. Soc.* **2001**, *123* (27), 6520−6526.
(57) Howard, S. T. Relationship between Basicity, Strain, and Intramolecular Hydrogen-Bond Energy in Proton Sponges. *J. Am. Chem. Soc.* **2000**, *122* (34), 8238−8244.

https://doi.org/10.1021/acsomega.3c05401
ACS Omega 2023, 8, 38546−38556